

See discussions, stats, and author profiles for this publication at: <https://www.researchgate.net/publication/263098064>

Relationship between β -relaxation and structural stability of lysozyme: Microscopic insight on thermostabilization mechanism by trehalose from Raman spectroscopy experiments

ARTICLE in THE JOURNAL OF CHEMICAL PHYSICS · JUNE 2014

Impact Factor: 2.95 · DOI: 10.1063/1.4882058 · Source: PubMed

CITATIONS

5

READS

15

3 AUTHORS, INCLUDING:



Alain Hédoux

Université des Sciences et Technologies de Li...

94 PUBLICATIONS 1,243 CITATIONS

SEE PROFILE



Yannick Guinet

Université des Sciences et Technologies de Li...

86 PUBLICATIONS 1,178 CITATIONS

SEE PROFILE

Relationship between α -relaxation and structural stability of lysozyme: Microscopic insight on thermostabilization mechanism by trehalose from Raman spectroscopy experiments

Alain Hédoux, Laurent Paccou, and Yannick Guinet

Citation: [The Journal of Chemical Physics](#) **140**, 225102 (2014); doi: 10.1063/1.4882058

View online: <http://dx.doi.org/10.1063/1.4882058>

View Table of Contents: <http://scitation.aip.org/content/aip/journal/jcp/140/22?ver=pdfcov>

Published by the [AIP Publishing](#)



Re-register for Table of Content Alerts

Create a profile.



Sign up today!



Relationship between β -relaxation and structural stability of lysozyme: Microscopic insight on thermostabilization mechanism by trehalose from Raman spectroscopy experiments

Alain Hédoux,^{a)} Laurent Paccou, and Yannick Guinet

Université Lille Nord de France, F-59000 Lille France, USTL UMET UMR 8207 F-59655 Villeneuve d'Ascq, France

(Received 11 February 2014; accepted 26 May 2014; published online 11 June 2014)

Raman investigations were carried out in the low-frequency and amide I regions on lysozyme aqueous solutions in absence and presence of trehalose. Raman spectroscopy gives the unique opportunity to analyze the protein and solvent dynamics in the low-frequency range while monitoring the unfolding process by capturing the spectrum of the amide I band. From the analysis of the quasielastic intensity, a dynamic change is firstly observed in a highly hydrated protein, around 70 °C, and interpreted in relation with the denaturation mechanism of the protein. The use of heavy water and partly deuterated trehalose gives clear information on protein–trehalose interactions in the native state of lysozyme (at room temperature) and during the thermal denaturation process of lysozyme. At room temperature, it was found that trehalose is preferentially excluded from the protein surface, and has a main effect on the tetrahedral local order of water molecules corresponding to a stiffening of the H-bond network in the solvent. The consequence is a significant reduction of the amplitude of fast relaxational motions, inducing a less marked dynamic transition shifted toward the high temperatures. Upon heating, interaction between trehalose and lysozyme is detected during the solvent penetration within the protein, i.e., while the native globular state softens into a molten globule (MG) state. Addition of trehalose reduces the protein flexibility in the MG state, improving the structural stability of the protein, and inhibiting the protein aggregation. © 2014 AIP Publishing LLC. [<http://dx.doi.org/10.1063/1.4882058>]

I. INTRODUCTION

Proteins are generally unstable in solutions and are susceptible to conformational changes when exposed to various stresses (high temperature, extreme pH, dehydration, and so on) during purification, processing, and storage. It is well known that co-solvents as disaccharides change the local structure of water¹ and its physical properties,² inducing the enhancement of the protein stability,³ in relation with the solute–water interactions. However, the main stabilization mechanism of proteins by disaccharides is often related to their preferential exclusion⁴ from the protein surface, leading to an excess of water in the first hydration shell, and then to a more compact native state. Disaccharides are also recognized as inhibitors of protein aggregation,⁵ mainly because of the reduction of the unfolded protein population, suggesting that aggregation is induced by protein unfolding. On the other hand, it has been considered that protein stabilizers inhibit aggregation because of the exclusion of cosolutes around the protein surface (preferential exclusion). However, it was shown that salts, preservatives, surfactants are added to protein solutions to prevent aggregation, that make it difficult to understand the mechanism for preservative-induced protein aggregation.

Analysis of model proteins^{6,7} have revealed a similar thermal denaturation process, with a crucial role of the solvent dynamics. From Raman investigations performed in the low-frequency region, it was found that the softening of the O–H intermolecular interactions in the solvent with temperature increase induced a less rigid tertiary structure, as it could be expected from the consideration of the coupling between protein and solvent dynamics.⁸ The analysis of the amide I band has shown that the dynamical change at temperatures above 60 °C leads to the solvent penetration within the protein, prior to the protein unfolding. From similar experiments in presence of trehalose, it was determined that trehalose strengthens intermolecular O–H interactions, stiffening and stabilizing the H-bond network of water upon heating.⁶ It was also shown that dissolving proteins in D₂O provides information on protein–solvent interactions during the process of protein denaturation, from the analysis of the amide I band position.

The present study focuses on the mechanism of protein stabilization by trehalose, from Raman investigations simultaneously carried out in the low-frequency range and in the amide I region. Firstly, the low-frequency analysis was extended to the very low-frequency range (5–30 cm^{−1}) in order to study fast relaxational motions. Secondly, Raman investigations were performed using trehalose and trehalose largely deuterated by freeze-drying a trehalose–D₂O solution. The amide I band mainly arises from C=O stretching vibrations with minor contributions of C–N stretching vibration and

^{a)} Author to whom correspondence should be addressed. Electronic mail: alain.hedoux@univ-lille1.fr

C–N–H bending motions.⁹ This latter is responsible for the sensitivity of the amide I band to NH/ND exchange in the protein backbone. It is also recognized that amide I band can be used to determine the secondary structure of proteins¹⁰ and to monitor protein unfolding induced by different kinds of stress.^{11,12} It was previously shown¹¹ that upon heating, the increase of conformational flexibility of lysozyme induced NH/ND exchanges in a molten globule state, prior to the unfolding process. New information on protein–solute interactions can be expected by comparing Raman data in the amide I region, obtained with trehalose and partially deuterated trehalose, in relation to the local mobility.

II. MATERIALS AND METHODS

A. Chemicals

Lysozyme (L, purity minimum 90%) and heavy water (isotopic purity of 99.99% atom D) were purchased from Sigma-Aldrich and used without further purification. High-purity anhydrous trehalose (T_h) was supplied from Sigma. Anhydrous trehalose was firstly dissolved in D_2O (W_d) to obtain T_hW_d mixtures, lysozyme was then dissolved in T_hW_d mixtures at a concentration of 10 wt. % of protein for 90 wt. % of T_hW_d . Anhydrous trehalose was freeze-dried after dissolution in 90 wt. % of D_2O in order to partly replace OH groups by OD groups in trehalose (T_d). Isotopic exchanges between trehalose and heavy water during freeze drying were determined by comparing intensities of O–H and O–D stretching bands in the freeze-dried product. The amount of deuteration was estimated by calculating the ratio $\frac{I_{OD}}{I_{OH}+I_{OD}} \approx 82\%$. The same freeze-dried product was used in all experiments performed with deuterated trehalose. Figure 1 shows the Raman spectrum in the intramolecular OH and OD stretching regions, for both solvents W_dT_h40 and W_dT_d40 . It is clearly observed that the integrated intensity in the OH region is significantly lowering for W_dT_d40 than for W_dT_h40 , indicating a large deuteration of trehalose.

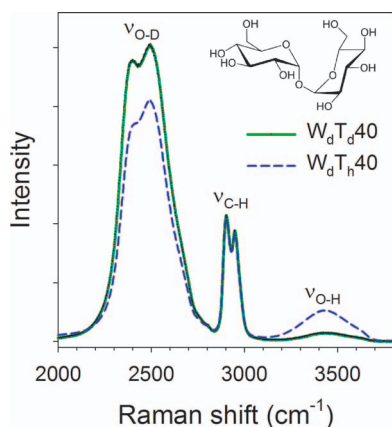


FIG. 1. Raman spectrum of intramolecular O–H and O–D stretching vibrations of commercial trehalose/ D_2O (W_dT_h40) and partly deuterated trehalose/ D_2O (W_dT_d40) mixtures. Both solutions are composed of 40 wt. % of trehalose. The structural conformation of trehalose is plotted in the top right of the figure.

B. Instruments

Raman spectra were recorded in the 5–200 cm^{-1} range, in VV+VH geometry to obtain non-polarized light-scattering spectrum under a scattering angle $\theta = 180^\circ$, using the 514.5 nm line of a mixed argon-krypton Coherent laser. The spectrometer is composed of a double monochromator comprising four mirrors characterized by a focal length of 800 mm and a spectrograph. The entrance and exit slits are opened and kept to 200 μm , determining the incident radiation a resolution nearly 2 cm^{-1} in the low-frequency range. It is the monochromator which prohibits the exciting line from entering the spectrograph field. The well-adapted positioning of the monochromator with respect to the spectrograph and the choice of experimental conditions (incident radiation, slit width) allow a rejection of exciting light down to 5 cm^{-1} . The spectrometer is equipped with a liquid nitrogen cooled charge coupled device detector. The high sensitivity of the detector and the large analyzed scattered volume ($\sim 0.4 cm^3$) allow us to record low-frequency Raman spectra in the 5–350 cm^{-1} range in 5 min. Solutions ($\sim 0.4 cm^3$) were loaded in spherical pyrex cell and hermetically sealed.

C. Data analysis

The spectrum of amide I (AmI) band is normalized by the integrated intensity in the 1500–1800 cm^{-1} range. The position of the AmI band is determined from a fitting procedure described in supplementary material.¹³ Physical stability of lysozyme is monitored by the position of AmI band, that is mainly dependent on the C=O...H hydrogen bonds within the secondary structure, i.e., dependent on the folded or unfolded state. Hydrogen bonds break down with unfolding of the secondary structure, making harder C=O stretching vibrations. As a consequence, the AmI position shifts toward the high frequencies during the unfolding process. At a given temperature, the position of AmI band reflects the equilibrium between populations of folded and unfolded conformational states, characterized by the equilibrium constant $K = (\omega_N - \omega) / (\omega - \omega_D)$. In this context, the unfolding process can be analyzed from the plot of the AmI band shift against temperature, in terms of change in the Gibbs free energy $\Delta G_{ND} = -RT \ln K$, where R is the gas constant, ω_N and ω_D are AmI positions in the native and denatured states.

The low-frequency Raman intensity is firstly converted into reduced intensity according to

$$I_r(\omega) = I_{Raman}(\omega) / ([n(\omega) + 1]\omega) \quad (1)$$

with $n(\omega) = [1 - \exp(\hbar\omega/kT)]^{-1}$, in order to obtain a low-frequency Raman spectrum free of band shape distortion due to thermal population effects. The reduced spectrum of a LW_d solution at room temperature is plotted in Figure 2. It is typical of a disordered molecular compound,¹⁴ characterized by the overlap of 2 contributions (in the 5–80 cm^{-1} range) corresponding to relaxational and vibrational motions. (i) the quasi-elastic scattering (I_{QES}) is the dominant contribution in the 5–30 cm^{-1} range. It corresponds to β -fast relaxational motions, and is related to the term $\langle u^2 \rangle_{rel}$.^{15,16} (ii) The

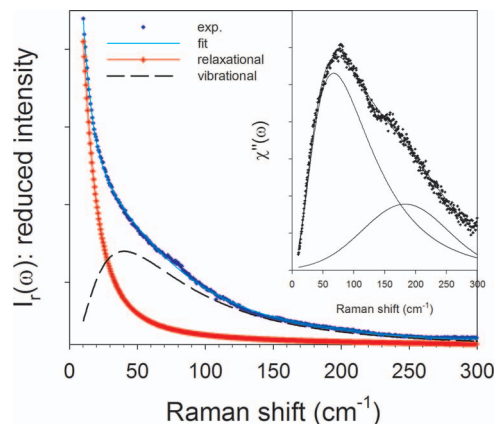


FIG. 2. Representations of the low-frequency Raman spectrum of a lysozyme aqueous solution (LW_d) at room temperature, and the corresponding fitting methods: reduced intensity ($I_r(\omega)$) and Raman susceptibility ($\chi''(\omega)$) in the inset.

vibrational intensity (I_{vib}) is related to $\langle u^2 \rangle_{vib}$ ¹⁶ and mainly corresponds to collective motions. It is recognized that low-frequency motions $\langle u^2 \rangle$ can be presented as the sum of vibrational and relaxational terms ($\langle u^2 \rangle = \langle u^2 \rangle_{vib} + \langle u^2 \rangle_{rel}$).¹⁶ It is also recognized that the vibrational component has nearly harmonic behavior $\langle u^2 \rangle_{vib} \sim kT$, while $\langle u^2 \rangle_{rel}$ increases with temperature much faster. The temperature dependence $\langle u^2 \rangle_{rel}(T)$ obtained by Raman spectroscopy was found to be similar to that determined by neutron scattering¹⁷ and inversely related to the temperature dependence of viscosity.^{16,18} The first contribution (i) corresponds to local anharmonic motions or fluctuations of individual atoms or groups of atoms, while the second contribution (ii) corresponds to global harmonic motions. Protein flexibility is associated with conformational fluctuations, and intimately related to the ability of proteins to undergo conformational changes.

The separated contributions of I_{QES} and I_{vib} can be obtained from a fitting procedure of the reduced spectrum (described in Figure 2), by using a lorentzian function centered at $\omega = 0$ to represent the contribution of I_{QES} , and a lognormal function for I_{vib} . In order to plot the temperature dependence of I_{QES} , the reduced intensity is normalized by the integrated intensity in the 70–170 cm^{-1} range, where the dominant contribution (I_{vib}) to the spectrum is weakly temperature dependent since it corresponds to quasi-harmonic motions. I_{QES} was then determined by integrating the normalized intensity in the 10–30 cm^{-1} range, where I_{vib} has a weak contribution.

After removing the I_{QES} contribution, I_{vib} is transformed into Raman susceptibility ($\chi''(\omega)$) according to

$$\chi''(\omega) = \omega \cdot I_{vib}(\omega) = \frac{C(\omega)}{\omega} G(\omega), \quad (2)$$

where $C(\omega)$ and $G(\omega)$, respectively, correspond to the light-vibration coupling coefficient and to the vibrational density of state (VDOS) usually determined by inelastic neutron scattering. It was found that $\chi''(\omega)$ is a close representation of the VDOS¹⁴ corresponding to collective quasi-harmonic motions for small and rigid molecules in disordered states. For larger and more flexible molecules, intramolecular motions overlap with the VDOS. The inset of Figure 2 shows that $\chi''(\omega)$ spec-

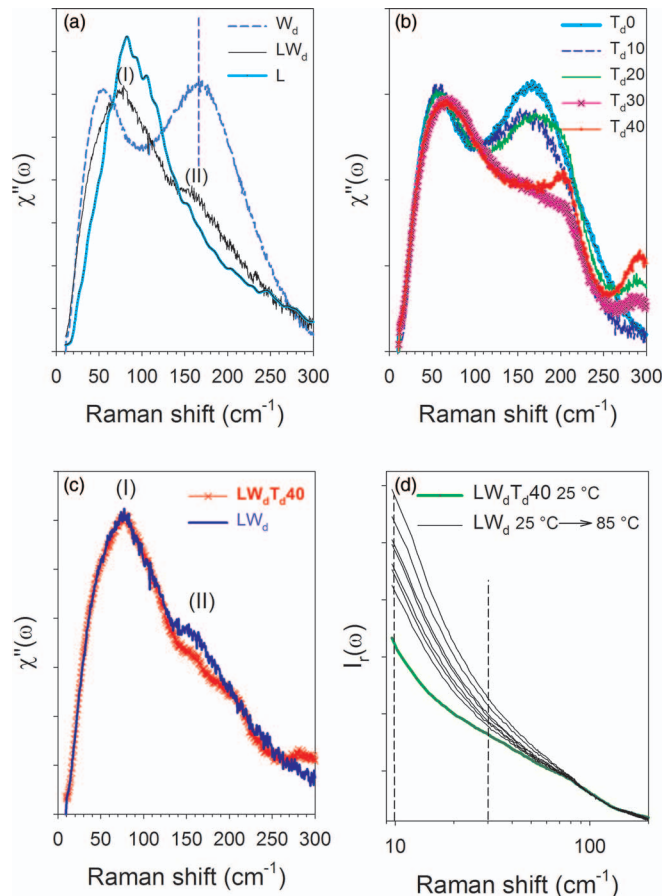


FIG. 3. Pannels of low-frequency Raman spectra of separated or mixed lysozyme-water-trehalose components. (a) Comparison of $\chi''(\omega)$ spectra of heavy water (W_d), lysozyme dissolved in heavy water with a concentration of 10 wt. % of lysozyme (LW_d) and dry lysozyme (L), used for the interpretation of bands (I) and (II) in LW_d solution. (b) $\chi''(\omega)$ spectra at room temperature of trehalose- D_2O mixtures, for weight fractions of trehalose ranging between 0 and 40 wt. % (c) $\chi''(\omega)$ spectra at room temperature of lysozyme dissolved in heavy water (LW_d) and dissolved in the mixture composed of heavy water and 40 wt. % of partly deuterated trehalose (LW_dT_d40). (d) Temperature dependence of the normalized reduced intensity in the LW_d solution between 25 and 85 °C by step of 10 °C. The spectrum at 25 °C is compared to that obtained in the LW_dT_d40 solution; the vertical dashed lines indicate the domain of integration to determine I_{QES} .

trum of an aqueous solution of lysozyme is composed of two broadbands. The assignment of these bands can be performed by comparing the spectrum of the aqueous protein solution (LW_d) with those of the solvent (W_d) and dry lysozyme (L) in Figure 3. Figure 3 indicates that the Raman susceptibility of D_2O is also composed of two broadbands. The low-frequency band is usually attributed to quasi-harmonic vibrations that atoms experience within the cage formed by their neighbors,^{19,20} the so-called caging effect. This band is also called Boson peak by some authors,^{8,21} by analogy with the low-frequency band in glassy states interpreted as resulting from the confinement of vibrations in nanodomains.²² The high-frequency band has been ascribed to collective intermolecular O-H...O stretching vibrations.^{11,20} The low-frequency band in the LW_d spectrum (band I) is clearly shifted toward the high frequencies to the spectrum of neat water, indicating a stiffening of the cage with the addition of lysozyme. In comparison with the spectrum of dry lysozyme

the spectrum of lysozyme solution (LW_d) exhibits a distinct peak around 170 cm^{-1} (band II), corresponding to the high-frequency band in the spectrum of neat water, and the low-frequency peak (band I) is significantly broadened reflecting the coupling between the protein and solvent dynamics. Consequently, band I in the spectrum of lysozyme solution can be interpreted as mainly corresponding to the quasi-harmonic lysozyme dynamics with a minor contribution of the coupling between protein and solvent dynamics, and band II corresponds to the intermolecular O–H stretching vibrations in the H-bond network of the solvent.

III. RESULTS

A. Analysis of the physical stability monitored by amide I (AmI) band

The thermal denaturation was firstly analyzed in the region of the amide I band in absence of trehalose, and in presence of 40% of commercial anhydrous trehalose (W_dT_h40) and 40% of largely deuterated trehalose (W_dT_d40), by freeze-drying of trehalose in D_2O . The temperature dependence of the position of the AmI band is plotted in Figure 4 for lysozyme dissolved in W_d , W_dT_h40 , and in W_dT_d40 mixtures. At room temperature, in comparison with the position of AmI in a solution of lysozyme dissolved in H_2O (LW_h , dashed line in Figure 4) the position of AmI for LW_d , LW_dT_h40 , and LW_dT_d40 solutions is identically shifted toward the low frequencies ($\Delta\omega_1$). This downshift is interpreted as resulting from isotopic exchange, around the protein surface, between OD groups of the solvent and NH groups of lysozyme exposed to the solvent. Upon heating, a second downshift ($\Delta\omega_2$) is systematically observed for LW_d , LW_dT_h40 , and LW_dT_d40 , but has not been observed when lysozyme was dissolved in H_2O .¹¹ This enhancement of isotopic exchange was previously interpreted as the signature of the solvent penetration

within the tertiary structure. This downshift of the AmI band is, therefore, a consequence of the transformation of the globular native state of the protein into the intermediate molten globule (MG) state, prior the unfolding process, in agreement with previous studies.^{11,23,24} The MG state corresponds to a more flexible tertiary structure,²⁵ where structural fluctuations of local and sub-global elements expose to the solvent, peptide amide protons which are buried in the native globular state. The present study reveals that the second downshift is deeper for the LW_d and LW_dT_d40 solutions than for LW_dT_h40 ($\Delta(\Delta\omega_2) \sim 2\text{ cm}^{-1}$), providing new information on the bio-preservation mechanism. Indeed, it is the indication of direct interactions between trehalose and lysozyme, not existing at room temperature. The identical level of isotopic exchanges at room temperature (similar frequencies of AmI band) in presence of normal or partly deuterated trehalose indicates that trehalose is preferentially excluded from the protein surface, in agreement with the hypothesis of preferential hydration,^{4,26} while at higher temperatures, the $\Delta(\Delta\omega_2)$ difference determined for both kinds of trehalose is the clear signature of interaction between trehalose and newly exposed amide protons in the MG state.

The unfolding process is detected by the shift of the AmI band toward the high frequencies, induced by the breakdown of intramolecular $C=O \cdots H-N$ hydrogen-bonds within helices making harder $C=O$ stretching vibrations. Unfolding curves are fitted using a sigmoidal function,

$$\omega = \omega_D + [(\omega_N - \omega_D)/(1 + \exp((T - T_m)/\Delta T))], \quad (3)$$

where ω_N and ω_D are AmI positions in the native and denatured states, and T_m strictly corresponds to the midpoint temperature of lysozyme unfolding.¹¹ The change in values of T_m (from 79.8°C in absence of trehalose to 87.4°C in presence of trehalose) determined by the fitting procedure indicates a stabilizing effect of trehalose. The comparison of the plots of AmI band positions corresponding to the LW_d and LW_dT_d40 solutions shows a deviation with respect to each other, mainly from the MG state, indicating that the stabilizing effect of trehalose is related to interaction between trehalose and lysozyme. The effect of trehalose on the structural stability of lysozyme can be estimated by calculating the change in Gibbs free energy from the fitting curves of AmI positions in LW_d and LW_dT_d40 solutions. Both corresponding ΔG_{ND} curves are plotted in the inset of Figure 4. The arrow shows the enhancement of ΔG ($\sim 10\text{ kJ/mole}$) in presence of trehalose, at $T_m = 79.7^\circ\text{C}$, in the LW_d solution, i.e., at the temperature of equal unfolded and folded populations ($\Delta G_{ND} = 0$) in the absence of trehalose. It is worth noting that the transformation of the native globular state into the MG state and the unfolding process cannot be discriminated by calorimetric experiments, since only one endotherm of denaturation is detected upon heating.^{11,24} Consequently, the midpoint temperature (T_m) determined by Differential Scanning Calorimetry (DSC) cannot be considered as corresponding to the equal folded and unfolded populations. Only spectroscopic investigations give information on the physical state of proteins by probing the secondary structure.

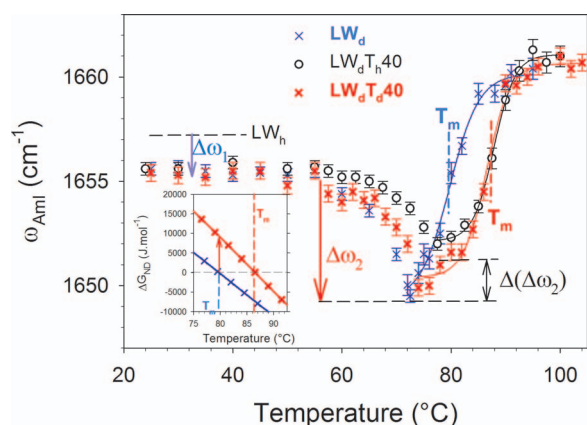


FIG. 4. Temperature dependence of the position of amide I (AmI) band in lysozyme dissolved in heavy water (LW_d), in a mixture of heavy water and 40 wt. % of commercial anhydrous trehalose (LW_dT_h40), and in a mixture of heavy water and 40 wt. % of partly deuterated trehalose (LW_dT_d40). The horizontal dashed line indicates the position of AmI band in a solution of lysozyme dissolved in H_2O (LW_h), and the full lines correspond to fitting procedures of lysozyme unfolding using sigmoidal shape (3). The change in the free Gibbs energy of lysozyme solutions in absence and in presence of trehalose is plotted in the inset. The arrow indicates the stabilizing effect of trehalose.

B. Analysis of the protein dynamics from low-frequency Raman spectrum

The influence of trehalose on the LFERS of water (D_2O) is firstly investigated. $\chi''(\omega)$ -spectra of trehalose–water solutions, for weight fractions of trehalose ranging between 0 and 40 wt. %, are plotted in Figure 3(b). The effect of trehalose on the low-frequency band is only detected from a concentration of 30 wt. %. Addition of trehalose induces a shift of the first band toward the high frequencies, corresponding to the stiffening of the cage experienced by water atoms. In contrast, trehalose induces the intensity decrease of the second band, accompanied with a high-frequency shift from a concentration of 10 wt. %, but drastically amplified above 30%. These spectral modifications indicate structural changes in the tetrahedral local organization of water molecules with a strengthening of intermolecular O–H interactions.

In a second step, the influence of trehalose on lysozyme solutions was analyzed, by comparing $\chi''(\omega)$ -spectra of lysozyme dissolved in D_2O (LW_d) and lysozyme dissolved in W_dT_d40 solution (LW_dT_d40) in Figure 3(c). Interestingly, Figure 3(c) shows that both spectra are strictly superimposed between 10 and 135 cm^{-1} , contrasting to the comparison between spectra of W_d and W_dT_d40 solutions, plotted in Figure 3(b). This indicates that trehalose has no influence on the vibrational dynamics of the protein, reflecting the absence of trehalose-lysozyme interaction at room temperature, in agreement with the preferential hydration hypothesis. At higher frequencies, the second peak (II) of the LW_dT_d40 solution has different characteristics (intensity, frequency) from that of the LW_d solution, in agreement with $\chi''(\omega)$ -spectra of trehalose solutions plotted in Figure 3(b), confirming that trehalose changes the local organization of water molecules.

The temperature dependences of frequencies of both bands (I) and (II), determined for LW_d and LW_dT_d40 solutions during the thermal denaturation process, are plotted in Figures 5(a) and 5(b). Figures 5(a) and 5(b) show the softening of the protein and solvent dynamics in the LW_d solution, upon heating from a temperature where AmI band downshifts ($\sim 60^\circ\text{C}$). In presence of 40 wt. % of trehalose the frequency of intermolecular O–H stretching vibrations is

significantly higher than that determined in the LW_d solution, and is roughly temperature independent. Around room temperature the first peak (I) is located at similar frequency for LW_d and LW_dT_d40 , as expected from Figure 3(c). However, above 60°C the frequency of peak I is systematically higher in LW_dT_d40 than in LW_d .

Figure 3(d) shows the temperature dependence of the reduced intensity in absence of trehalose. Spectra collected in LW_d and LW_dT_d40 lysozyme solutions are compared at room temperature. It is clearly observed in Figure 3(d) that trehalose reduces the amplitude of fast local motions. The quasielastic intensity is calculated in $10\text{--}30\text{ cm}^{-1}$ range characterized by the vertical dashed lines in Figure 3(d). The temperature dependences of I_{QES} are plotted in Figure 5(c) for both LW_d and LW_dT_d40 solutions. I_{QES} corresponds to fast anharmonic motions, i.e., the dynamics fluctuations $\langle u^2 \rangle_{rel}$ imposed by the solvent. In absence of trehalose, the temperature dependence of I_{QES} becomes stronger above 70°C , i.e., at the temperature corresponding to a minimum of $\omega_{AmI}(T)$. This feature observed in the high temperature range indicates a dynamical change. Such a phenomenon can be compared to the change of $\langle u^2 \rangle_{rel}(T)$, widely observed from neutron scattering experiments,^{27–29} in the low-temperature range²⁹ ($\sim 220\text{ K}$ in lysozyme²⁷), and called the dynamical transition. Since dynamical transition is not observed in dehydrated proteins, it has been related to the dynamics of the hydration shell.³⁰ The observation of a dynamical change at 70°C is in agreement with the detection of two dynamical transitions (at 220 K and 346 K) in lysozyme–water system³¹ with a low hydration level. The second dynamical change (above 346 K) was related to the dynamics of hydration water dominated by the non-hydrogen-bonded water molecules.³¹ In the high temperature range, the dynamical change observed in Figure 5(c) was associated with the Cp jump detected in calorimetric experiments.¹¹ A Cp jump is related to the release of conformational freedom degrees, as it can be usually observed at the glass transition between the solid amorphous state where the dynamics is frozen and the undercooled liquid. In the present case, it was previously associated with the transformation of the native globular state of the protein into a more flexible “molten globule” state.¹¹ Interestingly, it can

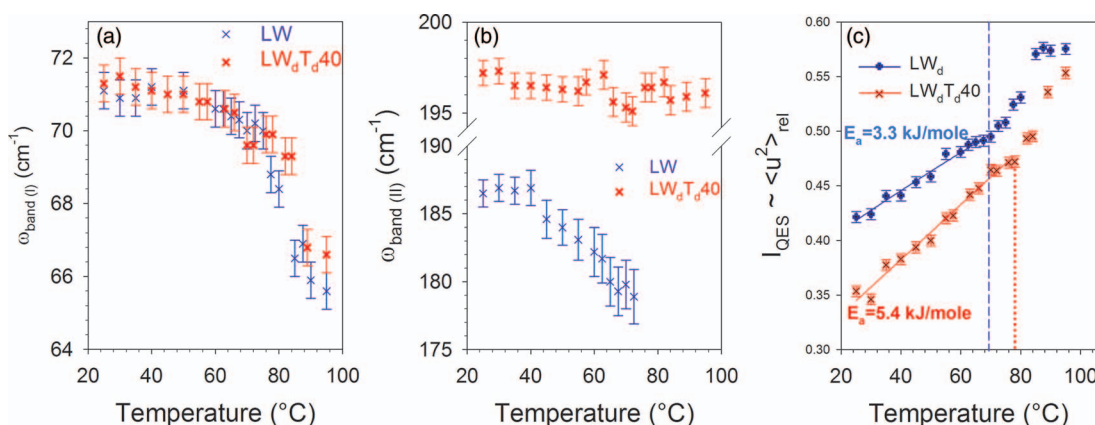


FIG. 5. Panels of the temperature dependences of dynamical parameters determined from the analysis of the low-frequency Raman spectrum of LW_d and LW_dT_d40 solutions; (a) frequency of band (I) in $\chi''(\omega)$ spectra; (b) frequency of band (II) in $\chi''(\omega)$ spectra; (c) quasi-elastic intensity (I_{QES}) determined by integration of normalized I_r spectra between 10 and 30 cm^{-1} .

be noticed that I_{QES} becomes temperature independent above 85 °C. It is an unusual temperature behavior of I_{QES} , indicating a limitation of anharmonicity upon heating which could be explained by the protein aggregation. The temperature independence of I_{QES} in the high temperature range could be interpreted as the signature of protein aggregation. Addition of trehalose induces a significant decrease of $\langle u^2 \rangle_{rel}$ and a shift toward the high temperatures of the change in the slope of $I_{QES}(T)$. In comparison with the $I_{QES}(T)$ -plot for the LW_d solution, the transition is less clearly observed in presence of 40 wt. % of trehalose, and the plateau of $I_{QES}(T)$ above 85 °C in the LW_d sample is not observed in the investigated temperature range. Consequently, trehalose limits the amplitude of fast local molecular motions in the native state at room temperature and at higher temperatures in the molten globule state. Relaxational motions are thermally activated and temperature dependences $\langle u^2 \rangle_{rel}(T)$ in both solutions were fitted using the Arrhenius law:

$$I_{QES} = A \cdot \exp\left(-\frac{E_a}{RT}\right), \quad (4)$$

where E_a is the activation energy. It is observed that in presence of trehalose, $\langle u^2 \rangle_{rel}$ is significantly lower and E_a is about 3 times higher than in absence of trehalose. It was shown that a decrease in $\langle u^2 \rangle_{rel}$ results from an antiplasticization effect in polymer materials,³² corresponding to the material stiffness. Consequently, addition of trehalose can be considered as corresponding to an antiplasticization effect in relation with β -relaxational motions, inducing a local stiffness within the tertiary structure which has a direct impact on local conformational flexibility.

IV. DISCUSSION

Raman spectroscopy gives the unique opportunity to analyze the protein and solvent dynamics in relation with the denaturation process, from low-frequency investigations simultaneously carried out with the analysis of the AmI band monitoring the protein unfolding. Calorimetric measurements,^{11,24,33} widely used to analyze protein denaturation, do not provide direct information on the physical state of the protein and on interactions between solvent and protein. The use of D_2O as solvent provides information on the description of the thermal denaturation process through the analysis of NH/ND isotopic exchange in helices. The downshift of the AmI band ($\Delta\omega_2$ in Figure 4), was considered as a signature of the solvent penetration within the tertiary structure, and the plot of $\omega_{AmI}(T)$ gives information on the transformation of the globular native tertiary structure into the “molten globule” state corresponding to a more flexible tertiary structure with intact secondary structure. In the present study, the influence of anhydrous trehalose (T_h) and deuterated trehalose (T_d) on the temperature dependence of AmI band is analyzed for the first time. This analysis reveals direct interactions between protein and disaccharide after the solvent penetration within the tertiary structure upon heating (above 6 °C), not existing in the globular native state of the protein at room temperature (see Figure 4). This can be explained by the existence of larger free volumes around the protein surface in the MG

state, making possible protein–sugar interactions. The analysis of the LFRS confirms that trehalose has no influence on the vibrational dynamics of the protein in its globular native state, in agreement with the preferential exclusion of the solute around the protein surface. On the other hand, trehalose distorts the tetrahedral local order of water molecules, making strengthened intermolecular O–H interactions, and then stiffening and stabilizing the H-bond network in the solvent at higher temperatures. By contrast to the vibrational dynamics, Figures 3(d) and 5(c) clearly show that addition of trehalose has a significant influence on β -relaxational dynamics at room temperature, probably imposed by the change in the solvent dynamics related to the distortion of the tetrahedral organization of water molecules.

The observation in Figure 5(c) of a dynamical change around 70 °C in absence of trehalose confirms the existence of two dynamical transitions,³¹ even for high hydration levels. Figure 5(b) clearly shows that at this temperature the frequency of the intermolecular O–H stretching vibrations becomes very low, indicating the softening of the H-bond network of water. In the present work, our investigations give a relation between the change in the relaxational protein dynamics and the softening of the H-bond network of water. The decrease in I_{QES} with addition of trehalose is probably induced by the stiffening of the H-bond network in the solvent and indicates that trehalose acts on water as an antiplasticizer for β -relaxational motions. The decrease in the internal mobility of a protein molecule is seen to stabilize it over a longer period of time. This result suggests that protein flexibility is inversely related to protein stability, as previously observed,³⁴ although the relation should be more complex.³⁵ In the case of freeze-dried proteins, it was found that the structural stability of proteins was directly related to β -relaxation processes of the sugar matrix.³⁶ For much higher hydration levels, we have shown here that the increase in local mobility upon heating can induce the exposition to the solvent of residues which were previously buried in the native globular state. The comparison of LW_dT_h40 and LW_dT_d40 solutions in Figure 4 shows direct interaction between trehalose and these residues, which is responsible for the structural stabilization of lysozyme by trehalose. Consequently, if preferential exclusion of trehalose around the protein surface has a crucial influence to stabilize the protein in its globular native state, the present study shows that trehalose-protein interactions stabilize the physical state of lysozyme in the MG state.

Figure 5(c) shows that trehalose inhibits the dynamical change in the high temperature range, and then reduces the protein flexibility in the MG state. It is recognized that MG states aggregate, since these states adopt a collapsed conformation that is more compact than the unfolded state, and are composed of large patches of contiguous surface hydrophobicity.³⁷ Consequently, interaction between trehalose and lysozyme in the MG state probably inhibits the protein aggregation, and the absence of plateau in the temperature dependence of I_{QES} could be considered as the experimental evidence of the non-aggregation of the protein induced by trehalose. If the consideration that this plateau is a signature of protein aggregation is adopted, the reduction of aggregation by trehalose can be attributed to direct interaction

between protein and trehalose in the molten globule state, reducing fast anharmonic motions of the protein.

V. CONCLUSION

The main contribution of Raman spectroscopy to the analysis of the mechanisms of protein denaturation/stabilization is to enable simultaneous investigations of the physical stability and the protein-solvent dynamics. The extension of low-frequency investigations in the domain of β -relaxational motions has revealed the existence of a second dynamic transition for high hydration levels of lysozyme, observed prior to protein unfolding. This result suggests causality between β -relaxational mobility and protein unfolding upon heating lysozyme solution. It is shown that trehalose has no influence on the vibrational dynamics of lysozyme, while trehalose significantly reduces the amplitude of β -fast relaxational motions, by changing the solvent dynamics. The use of D₂O, and normal and partly deuterated anhydrous trehalose provides information on protein-solvent interactions at the molecular level during the denaturation process, which cannot be obtained from neutron scattering and calorimetric experiments. Both low-frequency and AmI band analyzes confirm that trehalose is preferentially excluded from the protein surface at room temperature. However, the present investigations reveal that improving the stability of lysozyme in the high temperature range, by adding trehalose, is not explained by the preferential hydration model. Indeed, upon heating, direct interaction between lysozyme and trehalose is detected by comparing $\omega_{\text{AmI}}(T)$ curves for lysozyme solutions in absence and in presence of trehalose (deuterated and not). Interactions between lysozyme and trehalose are responsible for the enhancement of the protein stability by reducing the protein flexibility in the molten globule state, and then inhibit protein aggregation in the investigated temperature range (T_{room} up to about 100 °C). It was found that trehalose also acts on water, as anti-plasticizer, by distorting the tetrahedral local order of water and stiffening the H-bond network of the solvent. This has the effect of reducing the amplitude of fast protein motions from the coupling of solvent and protein dynamics. The presence of trehalose as co-solvent induces a lower protein flexibility and then a higher protein stability.

¹C. Branca, S. Magazu, F. Migliardo, and P. Migliardo, *Physica A* **304**(1-2), 314 (2002).

²S. Magazu, C. Branca, F. Migliardo, P. Migliardo, E. Vorobieva, and U. Vanderlingh, *Physica B* **301**(1-2) 134 (2001).

³R. Ionov, A. Hédoux, Y. Guinet, P. Bordat, A. Lerbret, F. Affouard, D. Prevost, and M. Descamps, *J. Non-Crystal. Solids* **352**, 4430 (2006).

⁴S. N. Timasheff, *Proc. Natl. Acad. Sci. U.S.A.* **99**(15), 9721 (2002).

⁵N. K. Jain and I. Roy, *Eur. J. Pharm. Biopharm.* **69**(3), 824 (2008).

⁶A. Hédoux, J. F. Willart, R. Ionov, F. Affouard, Y. Guinet, L. Paccou, A. Lerbret, and M. Descamps, *J. Phys. Chem. B* **110**, 22886 (2006).

⁷J.-A. Seo, A. Hedoux, Y. Guinet, L. Paccou, F. Affouard, A. Lerbret, and M. Descamps, *J. Phys. Chem. B* **114**, 6675 (2010).

⁸G. Caliskan, D. Mechtani, J. H. Roh, S. Azzam, M. T. Cicerone, S. Lin-Gibson, and I. Peral, *J. Chem. Phys.* **121**(4), 1978 (2004).

⁹W. K. Surewicz, H. H. Mantsch, and D. Chapman, *Biochemistry* **32**(2), 389 (1993).

¹⁰R. W. Williams and A. K. Dunker, *J. Mol. Biol.* **152**(4), 783 (1981).

¹¹A. Hédoux, R. Ionov, J. F. Willart, A. Lerbret, F. Affouard, Y. Guinet, M. Descamps, D. Prevost, L. Paccou, and F. Danède, *J. Chem. Phys.* **124**, 14703 (2006).

¹²A. Hédoux, S. Krenzelin, L. Paccou, Y. Guinet, M.-P. Flament, and J. Siepmann, *Phys. Chem. Chem. Phys.* **12**(40), 13189 (2010); A. Hédoux, Y. Guinet, and L. Paccou, *J. Phys. Chem. B* **115**, 6740 (2011).

¹³See supplementary material at <http://dx.doi.org/10.1063/1.4882058> for a description of the fitting procedure of amide I band.

¹⁴A. Hédoux, Y. Guinet, and M. Descamps, *Int. J. Pharm.* **417**, 17 (2011).

¹⁵G. Li, W. M. Du, X. K. Chen, H. Z. Cummins, and N. J. Tao, *Phys. Rev. A* **45**(6), 3867 (1992).

¹⁶A. P. Sokolov, E. Rössler, A. Kisliuk, and D. Quitmann, *Phys. Rev. Lett.* **71**(13), 2062 (1993); D. Quitmann, M. Soltwisch, and I. Petscherizin, *Prog. Theor. Phys.* **126**, 61 (1997).

¹⁷N. V. Surovtsev, J. A. H. Wiedersich, V. N. Novikov, E. Rossler, and A. P. Sokolov, *Phys. Rev. B* **58**(22), 14888 (1998).

¹⁸M. C. C. Ribeiro, *J. Chem. Phys.* **133**, 24503 (2010); A. Hédoux, Y. Guinet, L. Paccou, P. Derollez, and F. Danède, *ibid.* **138**, 214506 (2013); U. Buchenau and R. Zorn, *Europhys. Lett.* **18**, 523 (1992).

¹⁹A. Lerbret, F. Affouard, P. Bordat, A. Hedoux, Y. Guinet, and M. Descamps, *J. Chem. Phys.* **131**(24), 245103 (2009).

²⁰G. E. Walrafen, M. R. Fisher, M. S. Hokmabadi, and W. H. Yang, *J. Chem. Phys.* **85**(12), 6970 (1986).

²¹P. Lunkenheimer, U. Schneider, R. Brand, and A. Loidl, *Contemp. Phys.* **41**(1), 15 (2000).

²²T. Achibat, A. Boukenter, and E. Duval, *J. Chem. Phys.* **99**(3), 2046 (1993); L. Saviot, E. Duval, N. Surovtsev, J. F. Jal, and A. J. Dianoux, *Phys. Rev. B* **60**(1), 18 (1999); I. Pocsik and K. Koos, *Solid State Commun.* **74**(12), 1253 (1990).

²³P. L. Privalov, *J. Mol. Biol.* **258**(5), 707 (1996).

²⁴G. Salvetti, E. Tombari, L. Mikheeva, and G. P. Johari, *J. Phys. Chem. B* **106**(23), 6081 (2002).

²⁵I. H. van-Stokkum, H. Linsdell, J. M. Hadden, P. I. Haris, D. Chapman, and M. Bloemendal, *Biochemistry* **34**(33), 10508 (1995); V. Militello, C. Casarino, A. Emanuele, A. Giostra, F. Pullara, and M. Leone, *Biophys. Chem.* **107**(2), 175 (2004).

²⁶S. N. Timasheff, *Biochemistry* **41**(46), 13473 (2002).

²⁷S. Magazu, F. Migliardo, and A. Benedetto, *J. Phys. Chem. B* **115**, 7736 (2011).

²⁸W. Doster, S. Cusack, and W. Petry, *Nature (London)* **337**, 754-756 (1989); G. Zaccari, *Science* **288**(5471), 1604 (2000).

²⁹S. Capaccioli, K. Ngai, S. Ancherbak, and A. Paciaroni, *J. Phys. Chem. B* **116**, 1745 (2012).

³⁰W. Doster, S. Busch, and A. M. Gaspar, *Phys. Rev. Lett.* **104**, 98101 (2010).

³¹F. Mallamace, S.-H. Schen, M. Broccio, C. Corsaro, V. Crupi, D. Majolino, V. Venuti, P. Baglioni, E. Fratini, C. Vannucci, and H. E. Stanley, *J. Chem. Phys.* **127**, 045104 (2007).

³²D. S. Simmons and J. F. Douglas, *Soft Matter* **7**, 11010 (2011).

³³S. James and J. J. McManus, *J. Phys. Chem. B* **116**, 10182 (2012).

³⁴A. M. Tsai, T. J. Udovic, and D. A. Neumann, *Biophys. J.* **81**, 2339 (2001).

³⁵T. M. Kamerzell and C. R. Middaugh, *J. Pharm. Sci.* **97** (9), 3494 (2008).

³⁶M. T. Cicerone and J. F. Douglas, *Soft Matter* **8**, 2983 (2012).

³⁷E. Y. Chi, S. Krishnan, T. W. Randolph, and J. F. Carpenter, *Pharm. Res.* **20**(9), 1325 (2003); A. L. Fink, L. J. Calciano, Y. Goto, T. Kurotzu, and D. R. Palleros, *Biochemistry* **33**, 12504 (1994).